Molecular Therapy
Oncolytics
Original Article

AMERICAN SOCIETY of GENE & CELL THERAPY

Overexpression of Smac by an Armed Vesicular Stomatitis Virus Overcomes Tumor Resistance

Weike Li,[1,6] Ravi Chakra Turaga,[2,6] Xin Li,[2] Malvika Sharma,[2] Zahra Enadi,[1] Sydney Nicole Dunham Tompkins,[1] Kyle Christian Hardy,[1] Falguni Mishra,[2] Jun Tsao,[3] Zhi-ren Liu,[2] Daping Fan,[4] and Ming Luo[1,5]

[1]Department of Chemistry, Georgia State University, Atlanta, GA 30302, USA; [2]Department of Biology, Georgia State University, Atlanta, GA 30302, USA; [3]Vesta Biomedicals LLC, Atlanta, GA 30326, USA; [4]Department of Cell Biology and Anatomy, School of Medicine, University of South Carolina, Columbia, SC 29209, USA; [5]Center for Diagnostics and Therapeutics, Georgia State University, Atlanta, GA 30302, USA

Despite reports of successful clinical cases, many tumors appear to resist infection by oncolytic viruses (OVs). To circumvent this problem, an armed vesicular stomatitis virus was constructed by inserting a transgene to express Smac/DIABLO during virus infection (VSV-S). Endogenous Smac in HeLa cells was diminished during wtVSV infection, whereas the Smac level was enhanced during VSV-S infection. Apoptosis was readily induced by VSV-S, but not wtVSV, infection. More importantly, the tumor volume was reduced to a larger extent when xenografts of 4T1 cells in BALB/c mice and OV-resistant T-47D cells in nude mice were intratumorally injected with VSV-S. VSV-S represents a novel mechanism to overcome tumor resistance, resulting in more significant tumor regression due to enhanced apoptosis.

INTRODUCTION

Immune microenvironment of solid tumors plays a critical role in tumor progression. One of the approaches to exploit the immune system for cancer immunotherapy is to introduce oncolytic viruses (OVs) into the tumor. Since both the innate and adaptive immune systems are involved in cancer cell immunosurveillance and destruction, tumor infection by an OV may induce immune infiltration to alter the tumor microenvironment.[1] For breast cancer, clinical trials are in progress with T-VEC (an engineered herpes virus) (ClinicalTrials.gov: NCT02658812) and PeXa-VEC (an engineered vaccinia virus) (ClinicalTrials.gov: NCT02630368). While progress is being made, there are concerns about potential resistance to OVs by certain cancer types, especially by breast cancer.[2] A new generation of OVs has been generated by insertion of transgenes in the viral genome to express foreign genes during virus infection, including immune modulators and cytokines to enhance tumor lysis.[3,4]

One potential mechanism for tumor resistance to immunolysis by OVs may be inhibition of the cell death pathways. A family of proteins called inhibitor of apoptosis proteins (IAPs) may bind caspase-9 and -3 of the intrinsic pathway to inactivate them, or IAPs may ubiquitinylate other members in the extrinsic apoptotic pathway for lysosomal degradation.[5] IAPs are also shown to inhibit necroptosis and pyroptosis.[6] IAPs have long been recognized as targets for anticancer treatment or sensitizing agents.[7] To confirm that activities of IAPs represent the underlining mechanism of cancer resistance to therapy, we surveyed the gene expression database of human cancers (HuBase) generated by Crown Biosciences.[8] As shown in Figure 1A, mRNA levels of a number of IAPs, such as cIAP1 and XIAP, were elevated in various human cancers. This confirmed that the activities of IAPs have a fundamental relationship with therapy resistance by cancer cells.

Smac mimetics have been shown to sensitize tumor cells to OVs and other anticancer agents.[9–11] Oncolytic adenoviruses and vaccinia virus armed with Smac also greatly enhanced their antitumor effects.[12–16] Recently, it has been shown that combination of Smac mimetic and an OV resulted in synergistic enhancement of infiltration of $CD8^+$ T cells in immunosuppressed tumors.[17] After it is released from mitochondria, Smac interacts with various IAPs to release their inhibition of the intrinsic apoptotic pathway by allowing caspase-9 and caspase-3 to be activated.[18,19] IAP-induced ubiquitinylation of proteins involved in the extrinsic pathway may also be eliminated. Using the EMT6 breast carcinoma model in BALB/c mice, treatment by a Smac mimetic, LCL161, could reinvigorate exhausted $CD8^+$ T cells and polarize the tumor-associated macrophages toward M1-like macrophages. The synergistic effect of LCL161 with vesicular stomatitis virus ($VSV^{\Delta M51}$) is independent of the transforming growth factor α (TNF-α) pathway. The infection of EMT6 tumors by $VSV^{\Delta M51}$ induced cytokine and chemokine secretion that promotes $CD8^+$ T cell tumor infiltration. Acting as an adjuvant, infection of $VSV^{\Delta M51}$ led to a significant increase in EMT6-specific $CD8^+$ T cells in the tumor-draining lymph node when combined with LCL161. These results suggest that immune lytic activities of oncolytic VSV could be greatly enhanced by altering the tumor microenvironment.

To that end, we report here a design of a next-generation of oncolytic VSV. A transgene encoding Smac was directly inserted in the genome of VSV and a recombinant VSV was rescued, named VSV-S. We will

Received 15 August 2018; accepted 15 May 2019;
https://doi.org/10.1016/j.omto.2019.05.006.

[6]These authors contributed equally to this work.

Correspondence: Ming Luo, Department of Chemistry, Georgia State University, Atlanta, GA 30302, USA.
E-mail: mluo@gsu.edu

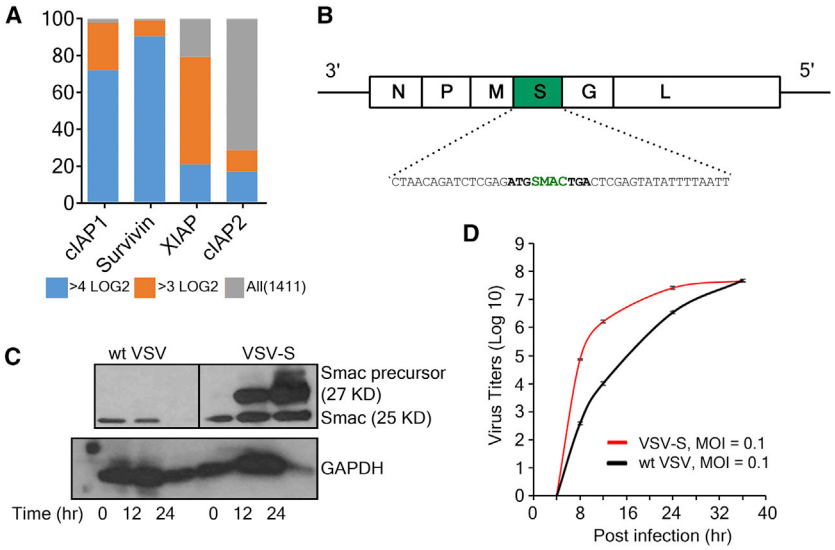

Figure 1. Generation of VSV-S

(A) mRNA levels of IAPs in human cancers. The database, HuBaseTM, constructed by Crown Biosciences, provided RNA sequencing (RNA-seq) data for all the cancer tissues collected. Data shows that 80% of tumors among 1,411 patient samples examined have 3LOG2 or higher levels of mRNA for cIAP1, Survivin, or XIAP, three key members in the IAP family. (B) Construction and propagation of armed vesicular stomatitis virus (VSV-S). Illustration of the genomic structure of VSV-S. Starting from the 3′ end, the five genes in the VSV genome are shown as white boxes labeled with N, P, M, G, and L. A green box labeled with S represents the transgene for the Smac precursor. The transgene was shown as a complimentary sequence with CT as a new gene junction. The positions of the first codon and the stop codon of the Smac precursor are also shown in bold letters. (C) Immunoblot analysis showing the expression of Smac in HeLa cells at 12 and 24 h after infection by wtVSV and VSV-S. mAb that recognizes both the full-length Smac and Smac (also known as Δ55 Smac) was used as the primary antibody. GAPDH was used as the reference control for protein levels in the cell lysates. (D) The growth curves of VSV-S and wtVSV in HeLa cells are plotted using virus titers at each time point. Experiments were performed in triplicates, and error bars represent mean ± SEM. The virus infection was initiated at an MOI of 0.1. The plaque-forming units were determined in HeLa cells.

show that VSV-S could be propagated to high titers and maintain the cellular level of Smac during VSV-S infection. The intrinsic pathway of apoptosis was clearly activated in breast cancer cell lines that express a higher level of IAPs.[20] In a xenograft model, up to 85% of tumor regression was observed by intratumoral injection of a single dose of VSV-S.

RESULTS

Generation of Smac-Armed VSV

The genome of VSV is a single-strand RNA enwrapped in the nucleocapsid. Starting at the 3′ end, there are five viral-encoded genes: N, P, M, G, and L for nucleocapsid, phosphoprotein, matrix, glycoprotein, and the L protein. There is a descending order of mRNA transcription levels from N to L, with about 30% reduction compared to the preceding gene.[21–24] The administration of Smac mimetic LCL161 must follow the intratumoral injection of $VSV^{\Delta M51}$ in order to show the synergistic antitumor effect.[17] This suggests that the reinvigoration of the immune response needs to be delayed until viral infection is established to synchronize the effects of the two mechanisms. In addition, the gene order in VSV genome is required for optimal viral growth.[25] Since the products of N, P, and M are required to be expressed proportionally for efficient viral replication and assembly, the transgene of Smac was chosen to be between M and G (Figure 1B). This location allows Smac to be expressed at a significant level well after the viral replication is established. After rescue of VSV-S by reverse genetics, its multi-cycle growth curve was compared to that of wild-type VSV (wtVSV) (Figure 1D). The final titer of VSV-S was similar to that of wtVSV, but its growth rate was little higher in the initial stage of infection. The average plaque size of VSV-S infection was larger than that of wtVSV (data not shown). The result indicated that insertion of Smac gene in VSV genome between M and G does not compromise VSV growth in cell culture.

Smac Level during VSV Infection

To confirm that expression of Smac was present during VSV-S infection, western blot was performed to detect Smac in VSV-S-infected HeLa cells. wtVSV was used as a control. In HeLa cells, endogenous mitochondrial Smac was detected before virus infection (Figure 1C). Smac is first expressed as a protein of 239 residues (precursor, 27 kDa), and then the mitochondria targeting signal of 55 residues is cleaved off from the N terminus of Smac precursor when it is bound in mitochondria.[18] Smac Δ55 has a molecular weight of 25 kDa. During infection of wtVSV, the endogenous Smac Δ55 was diminished after 12 hr of virus infection. The loss of endogenous Smac could be due to virus-induced mitophage.[26] As a consequence, cell death was restricted during 24 hr of wtVSV infection. On the other hand, the level of Smac Δ55 was elevated in VSV-S-infected HeLa cells. By 24 hr of VSV-S infection, a large percentage of infected cells died judging by the level of a housekeeping protein, glyceraldehyde 3-phosphate dehydrogenase (GAPDH). The result confirmed that Smac was highly expressed during VSV-S infection and cell death was more profound at 24 hr of VSV-S infection.

VSV-S Induces Apoptosis in Breast Cancer Cells

Breast cancer cell lines were tested for *in vitro* efficacy of VSV-S. The expression level of cIAP1, cIAP2, and Survivin in T-47D, MCF-7, MDA-MB-231, HCC-1143, and BT549 cells were screened. Cell killing by VSV-S was also measured (Figure 2). Levels of IAPs are clearly related to the resistance of wtVSV. VSV-S infection of these cells was more extensive than infection by wtVSV, including T-47D cells, which are also known to express very high levels of XIAP.[20] As shown in Figure 2C, T-47D cells were fully infected by wtVSV, and virus replication was active 24 hr after infection. A significant amount of wtVSV was produced in culture media (Figure 2D). However, the extent of cell death was limited. After 48 hr of infection,

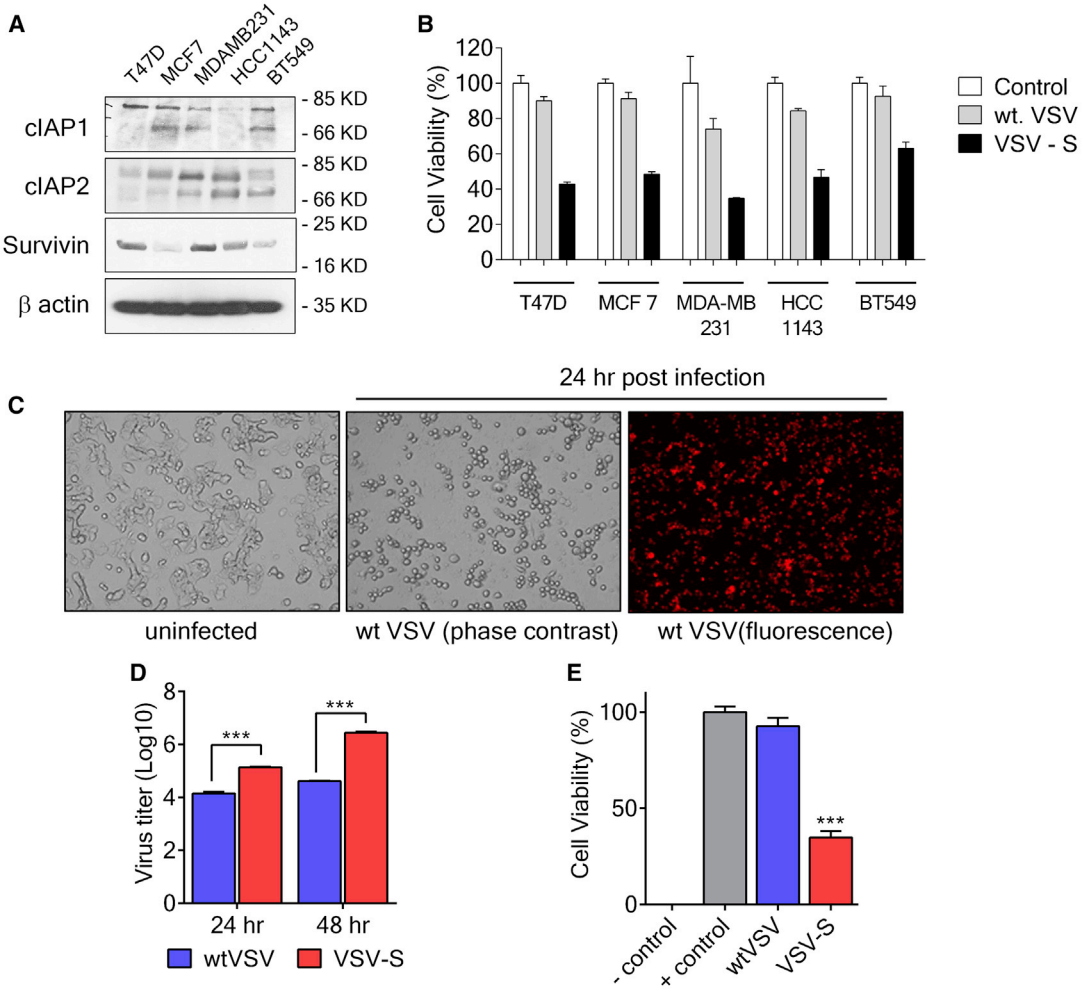

Figure 2. Overcoming Resistance in Breast Cancer Cells

(A) Immunoblot analysis showing levels of IAPs in different breast cancer cell lines including T-47D, MCF-7, MDA-MB-231, HCC-1143, and BT549. β-actin is the loading control. (B) Cell viability at 36 h after infection by VSV-S, wtVSV at MOI = 5, and uninfected control of various breast cancer cell lines tested in (A). Cell viability was evaluated by MTT assay. (C) Representative phase contrast and fluorescent images of T-47D cells after infection by VSV-S, wtVSV, and uninfected control after 24 h. wtVSV expresses an mCherry-fused P protein that labels the infected cells with red fluorescence (top right panel). T-47D cells infected by wtVSV appeared rounded up without any cell death. (D) Virus titers from infection of T-47D cells by wtVSV and VSV-S at 24 and 48 h postinfection. T-47D cells were infected at an MOI of 5.0 for each virus. (E) Viability of T-47D cells at 48 hr postinfection. MOIs of wtVSV and VSV-S were 5, and the cell viability was measured by the MTT assay. Error bars represent mean ± SEM and the significance in differences was determined by unpaired Student's t test.

less than 10% of T-47D cells were killed by wtVSV infection at MOI = 5 (Figure 2E). In contrast, infection of T-47D cells by VSV-S at MOI = 5 resulted in obvious cell death and production of about 10-fold more virus in culture media 24 hr after infection (Figures 2C and 2D). After 48 hr of infection, more than 60% of T-47D cells were killed by VSV-S infection, and about 100-fold more virus was produced in culture media (Figures 2D and 2E). The results showed that expression of Smac during VSV-S infection overcame the viral lysis resistance, leading to enhance cell killing and an increased production of progeny virus. Since Smac was diminished during wtVSV infection, it is likely that apoptosis of wtVSV-infected cells, specially via the intrinsic pathway, may be inhibited.

VSV-S Activates the Intrinsic Apoptotic Pathway

To check the extent of apoptosis induced by VSV-S in cells that express high levels of IAPs, MDA-MB-231 cells were infected with VSV-S, using wtVSV as a control. MDA-MB-231 cells express a high level of Survivin. At an MOI of 5 or higher, infection of VSV-S resulted in a much higher level of cell death than wtVSV (Figure 3A). The degree of virus-induced apoptosis was clearly higher in VSV-S-infected cells than wtVSV after 36 hr infection, based on the level of cleaved products of poly(ADP-ribose) polymerase (PARP), caspase-9, and caspase-3 (Figure 3B). To confirm that the intrinsic apoptosis pathway activated by VSV-S played a major role in causing cell death, infection of VSV-S was repeated in the presence of different

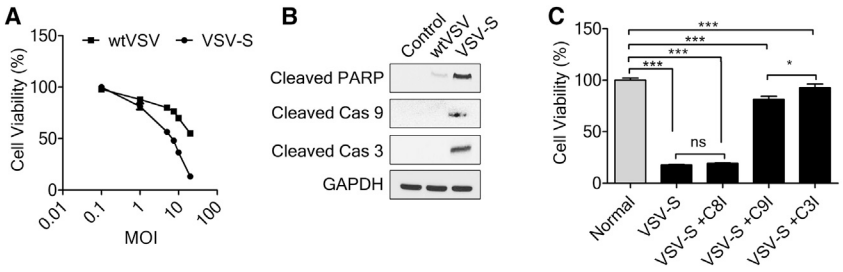

Figure 3. VSV-S Induces Apoptosis by Intrinsic Apoptotic Pathway

(A) Cell viability of MDA-MB-231 cells 36 h after infection by VSV-S versus wtVSV at different MOIs. (B) Immunoblot analysis of cleaved PARP, cleaved caspase-9, and cleaved caspase-3 in MDA-MB-231 cells. VSV-S infection induced apoptosis in MDA-MB-231 cells. wtVSV infection was used for the comparison, and uninfected cells were used as a control. (C) Cell viability of MDA-MB-231 cells 36 h after infection by VSV-S, in the presence of an inhibitor of caspase-8, caspase-9, or caspase-3. Error bars represent mean ± SEM. *$p < 0.05$, ***$p < 0.001$ by one-way ANOVA followed by post hoc Tukey's for multiple comparisons.

caspase inhibitors, including inhibitors of caspase-8, caspase-9, and caspase-3, respectively (Figure 3C). Cell death was greatly reduced in VSV-S infected MDA-MB-231 cells in the presence of a caspase-9 inhibitor or a caspase-3 inhibitor, whereas cell death was not affected by a caspase-8 inhibitor. The results confirmed that the intrinsic apoptosis pathway was responsible for the enhanced cell death caused by VSV-S infection.

VSV-S Demonstrates Tumor Regression *In Vivo*

In order to test the efficacy of designed VSV-S in *in vivo* systems, we first employed the 4T1 model, a very aggressive breast cancer model. 0.5×10^6 4T1 cells were implanted on to the right flank of BALB/c mice, and tumors were allowed to grow till ~150 mm^3 before starting the treatment. Tumor-bearing mice were randomly distributed, and intratumoral injections of vehicle, wtVSV, and VSV-S were given every third day (Figure 4A). Inhibition of tumor growth by VSV-S treatment was clearly more evident in tumor volume and tumor weight (Figures 4B and 4C). wtVSV also has an antitumoral effect, but not as significant as VSV-S. To analyze the effects on tumor, we carried out analyses on lysates prepared from tumors of vehicle-, wtVSV-, and VSV-S treated mice. Immunoblotting for cleaved caspase-3 indicated that there was a marked increase in apoptosis in VSV-S-treated mice compared to vehicle or wtVSV (Figure 4D). An increase in viral load was also observed when screened for viral protein N (VSV). We further tested VSV-S efficacy in T-47D cells implanted in immunocompromised mice. 1.0×10^6 T-47D cells were subcutaneously implanted into the right flank of each mouse. Mice were fed on water with estrogen. After about 6 weeks, tumors grew to 0.3 cm^3 or larger. VSV-S was intratumorally injected once in three tumors at a dosage of 1.0×10^5 plaque-forming units (PFU)/0.4 cm^3, and wtVSV was intratumorally injected once in two tumors at the same dosage. After 14 days, the tumors injected with VSV-S began to show signs of softness and shrinkage, while the tumors injected with wtVSV continued to grow. After 25 days, mice were euthanized and the tumors were excised for analyses. The tumor tissues were weighted, and their volumes were determined. The average regression of tumor volume was more than 85% upon a single intratumoral injection of VSV-S (Figure 4D. In contrast, tumor continued to grow after a single intratumoral injection of wtVSV. Activation of the intrinsic apoptosis pathway by VSV-S was clearly marked by cleaved caspase-3 (Figures 4E and 4F). The result clearly showed that VSV-S has a high capability to induce tumor regression upon intratumoral injection.

DISCUSSION

Immunotherapies with OVs and immune checkpoint inhibitors showed renewed promises for cancer treatment. However, many tumors are resistant to OVs[27–30] or fail to respond to checkpoint inhibitors.[31,32] When cells are infected by OVs, the virus replication causes tremendous stress on the host cells.[33] Cancer cells are usually developed under stress conditions, which may prepare these cells to resist stress to limit virus infection. Several strategies have been tested to exploit the synergetic effects of checkpoint inhibitors and OVs.[34–37] Other anticancer agents have also been used to sensitize cancer cells to OVs, including Smac mimetics.[11,38,39] Following the same strategy, we inserted a transgene after the M gene in VSV genome to express Smac during virus infection. The choice of the genomic location may regulate the level of transgene expression because the transcription descends when the position of the gene is more distal to the 3′ end of the genome.[40] Since N and M proteins are required in stoichiometric amounts in VSV virions, insertion of the transgene after the M gene would not tip over the balance between N and M proteins.

Our results revealed that endogenous Smac was diminished when HeLa cells were infected by wtVSV for 24 hr. The exact mechanisms of inhibition remain to be determined, but VSV has been shown to activate autophagy and ubiquitination to inhibit apoptosis.[41–43] On the other hand, the level of Smac in HeLa cells was maintained or enhanced throughout the 24-hr course of VSV-S infection (Figure 2). Apoptosis of HeLa cells was activated by VSV-S at 24 hr postinfection, as shown by the cleavage of caspase-3 (Figure 2). Activation of caspase-9 and caspase-3 were also clearly shown in VSV-S-infected MDA-MB-231 cells (Figure 3). When an inhibitor of caspase-9 or caspase-3 was added in the cell culture, cell killing by VSV-S was inhibited, but not by an inhibitor of caspase-8 (Figure 3), suggesting the cell killing by VSV-S was mainly through the intrinsic pathway. Our study demonstrated that expression of Smac by VSV-S sustained the level of Smac to mediate activation of caspase-3.

To test if VSV-S may overcome OV resistance of cancer cells, we infected breast cancer T-47D, MCF-7, MDA-MB-231, HCC-1143, and BT549cells. MDA-MB-231 is a triple negative (estrogen

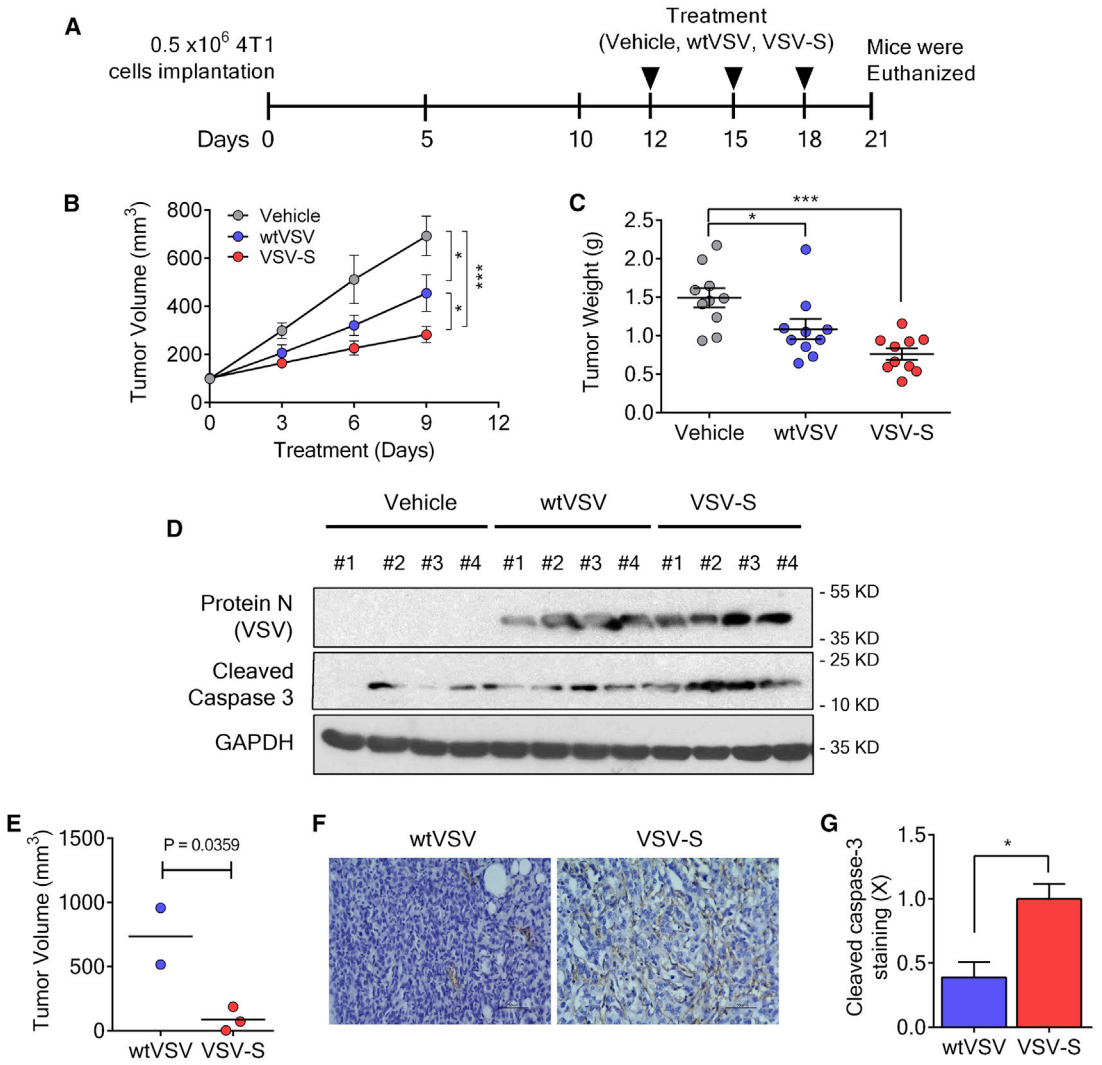

Figure 4. Tumor Reduction by Intratumoral Injection of VSV-S

(A) The scheme for implantation of 4T1 cells and treatment. (B) Tumor growth curves of 4T1 xenografts (n = 10) under treatment by intratumoral injection of vehicle (PBS, 30 μL), wtVSV (3.0×10^6 PFU in 30 μL of PBS, 5% sucrose), and VSV-S (3.0×10^6 PFU in 30 μL of PBS, 5% sucrose) at days 0, 3, and 6 (day 0 = 12 in A). (C) Tumor weight after three doses of treatment with respective agents. (D) Western blots indicating the expression of VSV protein N and cleaved caspase-3 in 4T1 tumors treated with respective agents. (E) Mean volume of xenografts of T-47D tumors at day 25 after intratumoral injection of VSV-S. The xenografts were generated by subcutaneous injection of 1.0×10^6 cells. Treatment was a single intratumoral infection of 100 μL VSV-S (1.0×10^5 PFU) per 0.4 cm^3. Injection of the same amount of wtVSV was used as a control. (F) Representative immunohistochemical images and (G) quantification of cleaved caspase-3 in the tumor of T-47D xenografts at the end of the treatment of wtVSV- or VSV-S-treated groups. Scale bars, 50 mm. Error bars represent mean ± SEM. *p < 0.05 by unpaired Student's t test.

receptor [ER], progesterone receptor [PR], and HER2 negative) breast cancer cell line expressing a high level of Survivin.[20,44] T-47D cells were isolated from a patient with an infiltrating ductal carcinoma of the breast and were shown to express a high level of XIAP.[20,45] When these cells were infected at an MOI of 5 or higher, cell killing by VSV-S infection is much higher than that by wtVSV infection. More than 60% of MDA-MB-31 cells was killed by VSV-S infection, in contrast to only 30% by wtVSV infection (Figure 2B). When T-47D cells were infected with wtVSV at an MOI of 5, most of the cells were infected (Figure 2C), consistent with previous observations that resistance to oncolytic VSV was not due to virus entry.[46] However, no significant cell death was observed when T-47D cells were infected by wtVSV even after 24 hr of infection (Figure 2). In contrast, more than 60% of T-47D cells were killed after infection by VSV-S (Figure 2B). The virus titers from infection of T-47D cells by VSV-S were also over 10-fold higher than those by wtVSV at 24 and 48 hr postinfection, respectively, at an MOI of 0.1 (Figure 2D). These observations indicate that VSV-S overcomes resistance of T-47D cells to spread more readily.

Table 1. Antibodies and Inhibitors

	Catalog No.	Vendor	Working Dilution
Inhibitors			
Caspase-8 inhibitor (Z-IETD-FMK)	FMK007	R&D Systems	50 nM
Caspase-9 inhibitor (Z-LEHD-FMK)	FMK008	R&D Systems	50 nM
Reagents (Antibodies)			
Anti-cIAP1	PA5-20066	Thermo Fisher	2 μg/mL
Anti-cIAP2	PA5-51700	Thermo Fisher	0.5 μg/mL
Anti-survivin	sc-17779	SCBT	1:300
Anti-GAPDH	sc-32233	SCBT	1:1,000
Anti-cleaved caspase-3	ab2302	Abcam	10 μg/mL
Anti-cleaved PARP1 [4B5BD2]	ab110315	Abcam	1:1,000
Anti-VSV N	rabbit polyclonal	Luo lab	1:5,000

After confirming that VSV-S overcomes T-47D resistance in cell culture, it is prudent to determine if VSV-S could overcome resistance of solid tumors. In fact, establishment of VSV infection in its natural host, cattle, is proven to be difficult unless inoculation was carried out by VSV-infected black fly (*Simulium vittatum*) bite at the coronary bands.[47] Spread of VSV infection in tumors may also be limited as well. A previous study showed that three consecutive intratumoral injections of 6.6×10^8 TCID50 VSV-interferon β (IFNβ)-sodium/iodide symporter (NIS) were required to demonstrate inhibition of tumor growth in a xenograft model.[48] This suggested that VSV-IFNβ-NIS could not spread productively in xenografts. It is also true for FDA-approved talimogene laherparepvec (T-VEC) that required three consecutive intratumoral injections of 1.0×10^8 PFU virus to show inhibition of tumor growth.[49] These may be the reasons that the current concept of OV treatment of cancer is more focused on immunotherapy than virotherapy, further augmented by the fact that both aforementioned viruses were armed to express immune stimulators, i.e., IFNβ and granulocyte-macrophage colony-stimulating factor (GM-CSF), respectively. However, virotherapy is still a viable approach if spread of OV in tumors can be established. Our *in vivo* findings in the 4T1 model have demonstrated a nearly 60% decrease in tumor progression and increased apoptosis in cancer cells treated with VSV-S. wtVSV also exhibited some antitumor potential, however not as significant as VSV-S. We also tested VSV-S in T-47D xenografts in nude mice that were intratumorally injected with a single dose of 1.0×10^5 PFU VSV-S per 0.4 cm^3; the volume of xenografts was reduced by more than 85% at 25 days after virus injection (Figure 4), whereas the injection of the same amount of wtVSV did not prevent tumor growth. Such dramatic tumor necrosis could only be possible if VSV-S could readily spread throughout the xenografts. We believe that Smac-armed VSV not only overcomes tumor resistance, but also is competent to spread in tumors productively. This outcome re-establishes that virotherapy with OVs is still a viable treatment approach as long as a productive spread of an OV could be established in tumors. However, comparisons of the outcomes from the immunocompetent 4T1 model versus the immunocompromised T-47D model suggest that the host immune system, especially the tumor microenviroment, may limit the spread of the OV within the tumor. 4T1 cells showed very low immunogenicity and did not respond to immunotherapy well.[17] Our results confirmed that VSV-S has more potent antitumoral activities by inducing apoptosis. Its therapeutic efficacy may be further improved through combination with immunotherapy or targeted therapy.

MATERIALS AND METHODS

Cell Lines

HeLa, T-47D, MCF-7, MDA-MB-231, HCC-1143, 4T1, and BT549 cell lines were obtained from ATCC. HeLa cells were grown in DMEM, supplemented with 10% fetal bovine serum (FBS). MDA-MB-231 cells were grown in DMEM, supplemented with 10% FBS. T-47D, MCF-7, HCC-1143, and BT549 cells were grown in RPMI-1640 medium, supplemented with 10% FBS and 0.2 units/mL insulin (7 μg/mL). All cells were grown at 37°C, 5% CO_2, in a humidified incubator. 4T1 cells were cultured in RPMI-1640 medium with 10% FBS.

Viruses

VSV-S was generated by reverse genetics.[50] The transgene of Smac was cloned in the VSV genome in the cDNA vector. Lipofectamine (Thermo Fisher Scientific) co-transfection of the VSV-S cDNA with plasmid-N (pN), plasmid-P (pP), and plasmid-L (pL) into BSR cells infected with vaccinia virus expressing T7 RNA polymerase, vTF7-3, rescued VSV-S. Vectors pN, pP, and pL express the nucleocapsid, phosphoprotein, and the L protein, respectively. wtVSV was also rescued by reverse genetics using the wild-type (WT) genomic cDNA. Recombinant viruses were plaque purified twice. Virus stocks were propagated in HeLa cells. To prepare viruses for *in vivo* studies, HeLa cells were grown in 150-mm dishes and infected with virus stock. Culture media from infected cells were collected 48 hr postinfection, and the virus was concentrated by ultracentrifugation. Virus pellets were resuspended in PBS containing 5% sucrose and stored in −80°C.

Virus Infection

Cells were washed with Dulbecco's PBS (DPBS), and the virus inoculum was added. Virus absorption was carried out for 1 hr at 37°C. After adding culture media without FBS, virus infection proceeded at 37°C, 5% CO_2, for designated hr. Virus titers by PFU were determined by plaque assays using HeLa cells.

Cell Viability

The viability was determined by CellTiter 96 non-radioactive cell proliferation assay 3-(4,5-dimethylthiazol-2-yl)-2,5-diphenyltetrazolium bromidefor (MTT) (Promega).

Antibodies in Western Blot and Caspase Inhibitors

The following antibodies were used in western blot: monoclonal rabbit anti-Smac (Epitomics), rabbit polyclonal anti-GAPDH (Abcam), rabbit polyclonal anti-cleaved PARP, anti-cleaved caspase-9,

anti-caspase-3, anti-cleaved caspase-3 (Cell Signaling Technology), and rabbit polyclonal anti-VSV N (custom-made for the Luo lab). Details of antibody and caspase inhibitor usage are listed in Table 1.

Animal Study

The experimental protocol was approved by IACUC of Georgia State University. 6-week-old BALB/c mice were purchased from the Jackson Laboratory. Xenografts were generated by subcutaneous injection of 0.5×10^6 4T1 cells in the flank of each mouse. 4-week-old nude mice were purchased from the Jackson Laboratory. Xenografts were generated by subcutaneous infection of 1.0×10^6 T-47D cells into the flank of each mouse. Researchers were blinded for the study groups.

AUTHOR CONTRIBUTIONS

W.L., R.C.T., J.T., D.F., and M.L. designed the experiments. W.L., R.C.T., X.L., Z.E., S.N.D.T., K.C.H., J.T., D.F., M.S., and M.L. performed the experiments. M.S. and F.M. participated xenograft experiment and histology analyses. W.L., R.C.T., J.T., D.F., Z.-r.L., and M.L. analyzed the results and wrote the manuscript.

CONFLICTS OF INTEREST

The authors declare no competing interests.

ACKNOWLEDGMENTS

This work has been supported in part by a grant to M.L. from the Georgia Research Alliance (GRA.VL18.G4).

REFERENCES

1. Nakasone, E.S., Hurvitz, S.A., and McCann, K.E. (2018). Harnessing the immune system in the battle against breast cancer. Drugs Context *7*, 212520.
2. Berkey, S.E., Thorne, S.H., and Bartlett, D.L. (2017). Oncolytic Virotherapy and the Tumor Microenvironment. Adv. Exp. Med. Biol. *1036*, 157–172.
3. Aurelian, L. (2016). Oncolytic viruses as immunotherapy: progress and remaining challenges. OncoTargets Ther. *9*, 2627–2637.
4. de Graaf, J.F., de Vor, L., Fouchier, R.A.M., and van den Hoogen, B.G. (2018). Armed oncolytic viruses: A kick-start for anti-tumor immunity. Cytokine Growth Factor Rev. *41*, 28–39.
5. Finlay, D., Teriete, P., Vamos, M., Cosford, N.D.P., and Vuori, K. (2017). Inducing death in tumor cells: roles of the inhibitor of apoptosis proteins. F1000Res. *6*, 587.
6. Silke, J., and Vince, J. (2017). IAPs and Cell Death. Curr. Top. Microbiol. Immunol. *403*, 95–117.
7. Rathore, R., McCallum, J.E., Varghese, E., Florea, A.M., and Busselberg, D. (2017). Overcoming chemotherapy drug resistance by targeting inhibitors of apoptosis proteins (IAPs). Apoptosis *22*, 898–919.
8. Jiang, J., Wang, D.D., Yang, M., Chen, D., Pang, L., Guo, S., Cai, J., Wery, J.P., Li, L., Li, H.Q., and Lin, P.P. (2015). Comprehensive characterization of chemotherapeutic efficacy on metastases in the established gastric neuroendocrine cancer patient derived xenograft model. Oncotarget *6*, 15639–15651.
9. Cai, J., Lin, Y., Zhang, H., Liang, J., Tan, Y., Cavenee, W.K., and Yan, G. (2017). Selective replication of oncolytic virus M1 results in a bystander killing effect that is potentiated by Smac mimetics. Proc. Natl. Acad. Sci. USA *114*, 6812–6817.
10. Beug, S.T., Pichette, S.J., St-Jean, M., Holbrook, J., Walker, D.E., LaCasse, E.C., and Korneluk, R.G. (2018). Combination of IAP Antagonists and TNF-α-Armed Oncolytic Viruses Induce Tumor Vascular Shutdown and Tumor Regression. Mol. Ther. Oncolytics *10*, 28–39.
11. Dobson, C.C., Naing, T., Beug, S.T., Faye, M.D., Chabot, J., St-Jean, M., Walker, D.E., LaCasse, E.C., Stojdl, D.F., Korneluk, R.G., and Holcik, M. (2017). Oncolytic virus synergizes with Smac mimetic compounds to induce rhabdomyosarcoma cell death in a syngeneic murine model. Oncotarget *8*, 3495–3508.
12. Wang, S.B., Tan, Y., Lei, W., Wang, Y.G., Zhou, X.M., Jia, X.Y., Zhang, K.J., Chu, L., Liu, X.Y., and Qian, W.B. (2012). Complete eradication of xenograft hepatoma by oncolytic adenovirus ZD55 harboring TRAIL-IETD-Smac gene with broad anti-tumor effect. Hum. Gene Ther. *23*, 992–1002.
13. Pan, Q.W., Zhong, S.Y., Liu, B.S., Liu, J., Cai, R., Wang, Y.G., Liu, X.Y., and Qian, C. (2007). Enhanced sensitivity of hepatocellular carcinoma cells to chemotherapy with a Smac-armed oncolytic adenovirus. Acta Pharmacol. Sin. *28*, 1996–2004.
14. Ge, Y., Lei, W., Ma, Y., Wang, Y., Wei, B., Chen, X., Ru, G., He, X., Mou, X., and Wang, S. (2017). Synergistic antitumor effects of CDK inhibitor SNS-032 and an oncolytic adenovirus co-expressing TRAIL and Smac in pancreatic cancer. Mol. Med. Rep. *15*, 3521–3528.
15. Baird, S.K., Aerts, J.L., Eddaoudi, A., Lockley, M., Lemoine, N.R., and McNeish, I.A. (2008). Oncolytic adenoviral mutants induce a novel mode of programmed cell death in ovarian cancer. Oncogene *27*, 3081–3090.
16. Pan, Q., Huang, Y., Chen, L., Gu, J., and Zhou, X. (2014). SMAC-armed vaccinia virus induces both apoptosis and necroptosis and synergizes the efficiency of vinblastine in HCC. Hum. Cell *27*, 162–171.
17. Kim, D.S., Dastidar, H., Zhang, C., Zemp, F.J., Lau, K., Ernst, M., Rakic, A., Sikdar, S., Rajwani, J., Naumenko, V., et al. (2017). Smac mimetics and oncolytic viruses synergize in driving anticancer T-cell responses through complementary mechanisms. Nat. Commun. *8*, 344.
18. Du, C., Fang, M., Li, Y., Li, L., and Wang, X. (2000). Smac, a mitochondrial protein that promotes cytochrome c-dependent caspase activation by eliminating IAP inhibition. Cell *102*, 33–42.
19. Verhagen, A.M., Ekert, P.G., Pakusch, M., Silke, J., Connolly, L.M., Reid, G.E., Moritz, R.L., Simpson, R.J., and Vaux, D.L. (2000). Identification of DIABLO, a mammalian protein that promotes apoptosis by binding to and antagonizing IAP proteins. Cell *102*, 43–53.
20. Foster, F.M., Owens, T.W., Tanianis-Hughes, J., Clarke, R.B., Brennan, K., Bundred, N.J., and Streuli, C.H. (2009). Targeting inhibitor of apoptosis proteins in combination with ErbB antagonists in breast cancer. Breast Cancer Res. *11*, R41.
21. Villarreal, L.P., Breindl, M., and Holland, J.J. (1976). Determination of molar ratios of vesicular stomatitis virus induced RNA species in BHK21 cells. Biochemistry *15*, 1663–1667.
22. Iverson, L.E., and Rose, J.K. (1981). Localized attenuation and discontinuous synthesis during vesicular stomatitis virus transcription. Cell *23*, 477–484.
23. Ball, L.A., and White, C.N. (1976). Order of transcription of genes of vesicular stomatitis virus. Proc. Natl. Acad. Sci. USA *73*, 442–446.
24. Abraham, G., and Banerjee, A.K. (1976). Sequential transcription of the genes of vesicular stomatitis virus. Proc. Natl. Acad. Sci. USA *73*, 1504–1508.
25. Ball, L.A., Pringle, C.R., Flanagan, B., Perepelitsa, V.P., and Wertz, G.W. (1999). Phenotypic consequences of rearranging the P, M, and G genes of vesicular stomatitis virus. J. Virol. *73*, 4705–4712.
26. Shulak, L., Beljanski, V., Chiang, C., Dutta, S.M., Van Grevenynghe, J., Belgnaoui, S.M., Nguyên, T.L., Di Lenardo, T., Semmes, O.J., Lin, R., and Hiscott, J. (2014). Histone deacetylase inhibitors potentiate vesicular stomatitis virus oncolysis in prostate cancer cells by modulating NF-κB-dependent autophagy. J. Virol. *88*, 2927–2940.
27. Felt, S.A., Droby, G.N., and Grdzelishvili, V.Z. (2017). Ruxolitinib and polycation combination treatment overcomes multiple mechanisms of resistance of pancreatic cancer cells to oncolytic vesicular stomatitis virus. J. Virol. *91*, e00461-17.
28. Ebrahimi, S., Ghorbani, E., Khazaei, M., Avan, A., Ryzhikov, M., Azadmanesh, K., and Hassanian, S.M. (2017). Interferon-Mediated Tumor Resistance to Oncolytic Virotherapy. J. Cell. Biochem. *118*, 1994–1999.
29. Lee, N.H., Kim, M., Oh, S.Y., Kim, S.G., Kwon, H.C., and Hwang, T.H. (2017). Gene expression profiling of hematologic malignant cell lines resistant to oncolytic virus treatment. Oncotarget *8*, 1213–1225.

30. Hastie, E., Cataldi, M., Moerdyk-Schauwecker, M.J., Felt, S.A., Steuerwald, N., and Grdzelishvili, V.Z. (2016). Novel biomarkers of resistance of pancreatic cancer cells to oncolytic vesicular stomatitis virus. Oncotarget *7*, 61601–61618.

31. Fang, X.N., and Fu, L.W. (2016). Predictive Efficacy Biomarkers of Programmed Cell Death 1/Programmed Cell Death 1 Ligand Blockade Therapy. Recent Patents Anticancer Drug Discov. *11*, 141–151.

32. Yuasa, T., Masuda, H., Yamamoto, S., Numao, N., and Yonese, J. (2017). Biomarkers to predict prognosis and response to checkpoint inhibitors. Int. J. Clin. Oncol. *22*, 629–634.

33. Camini, F.C., da Silva Caetano, C.C., Almeida, L.T., and de Brito Magalhães, C.L. (2017). Implications of oxidative stress on viral pathogenesis. Arch. Virol. *162*, 907–917.

34. Durham, N.M., Mulgrew, K., McGlinchey, K., Monks, N.R., Ji, H., Herbst, R., Suzich, J., Hammond, S.A., and Kelly, E.J. (2017). Oncolytic VSV Primes Differential Responses to Immuno-oncology Therapy. Molecular Ther *25*, 1917–1932.

35. Bastin, D., Walsh, S.R., Al Saigh, M., and Wan, Y. (2016). Capitalizing on Cancer Specific Replication: Oncolytic Viruses as a Versatile Platform for the Enhancement of Cancer Immunotherapy Strategies. Biomedicines *4*, E21.

36. Fend, L., Yamazaki, T., Remy, C., Fahrner, C., Gantzer, M., Nourtier, V., Préville, X., Quéméneur, E., Kepp, O., Adam, J., et al. (2017). Immune Checkpoint Blockade, Immunogenic Chemotherapy or IFN-α Blockade Boost the Local and Abscopal Effects of Oncolytic Virotherapy. Cancer Res. *77*, 4146–4157.

37. Russell, S.J., and Peng, K.W. (2017). Oncolytic Virotherapy: A Contest between Apples and Oranges. Molecular Ther *25*, 1107–1116.

38. Lei, W., Wang, S., Yang, C., Huang, X., Chen, Z., He, W., Shen, J., Liu, X., and Qian, W. (2016). Combined expression of miR-34a and Smac mediated by oncolytic vaccinia virus synergistically promote anti-tumor effects in Multiple Myeloma. Sci. Rep. *6*, 32174.

39. Beug, S.T., Conrad, D.P., Alain, T., Korneluk, R.G., and Lacasse, E.C. (2015). Combinatorial cancer immunotherapy strategies with proapoptotic small-molecule IAP antagonists. Int. J. Dev. Biol. *59*, 141–147.

40. Barr, J.N., Whelan, S.P., and Wertz, G.W. (2002). Transcriptional control of the RNA-dependent RNA polymerase of vesicular stomatitis virus. Biochim. Biophys. Acta *1577*, 337–353.

41. Choi, Y.B., Shembade, N., Parvatiyar, K., Balachandran, S., and Harhaj, E.W. (2016). TAX1BP1 Restrains Virus-Induced Apoptosis by Facilitating Itch-Mediated Degradation of the Mitochondrial Adaptor MAVS. Mol. Cell. Biol. *37*, e00422-16.

42. Malilas, W., Koh, S.S., Lee, S., Srisuttee, R., Cho, I.R., Moon, J., Kaowinn, S., Johnston, R.N., and Chung, Y.H. (2014). Suppression of autophagic genes sensitizes CUG2-overexpressing A549 human lung cancer cells to oncolytic vesicular stomatitis virus-induced apoptosis. Int. J. Oncol. *44*, 1177–1184.

43. García-Valtanen, P., Ortega-Villaizán, Mdel.M., Martínez-López, A., Medina-Gali, R., Pérez, L., Mackenzie, S., Figueras, A., Coll, J.M., and Estepa, A. (2014). Autophagy-inducing peptides from mammalian VSV and fish VHSV rhabdoviral G glycoproteins (G) as models for the development of new therapeutic molecules. Autophagy *10*, 1666–1680.

44. Cailleau, R., Young, R., Olivé, M., and Reeves, W.J., Jr. (1974). Breast tumor cell lines from pleural effusions. J. Natl. Cancer Inst. *53*, 661–674.

45. Shiu, R.P. (1980). Processing of prolactin by human breast cancer cells in long term tissue culture. J. Biol. Chem. *255*, 4278–4281.

46. Carey, B.L., Ahmed, M., Puckett, S., and Lyles, D.S. (2008). Early steps of the virus replication cycle are inhibited in prostate cancer cells resistant to oncolytic vesicular stomatitis virus. J. Virol. *82*, 12104–12115.

47. Reis, J.L., Jr., Rodriguez, L.L., Mead, D.G., Smoliga, G., and Brown, C.C. (2011). Lesion development and replication kinetics during early infection in cattle inoculated with Vesicular stomatitis New Jersey virus via scarification and black fly (Simulium vittatum) bite. Vet. Pathol. *48*, 547–557.

48. Patel, M.R., Jacobson, B.A., Ji, Y., Drees, J., Tang, S., Xiong, K., Wang, H., Prigge, J.E., Dash, A.S., Kratzke, A.K., et al. (2015). Vesicular stomatitis virus expressing interferon-β is oncolytic and promotes antitumor immune responses in a syngeneic murine model of non-small cell lung cancer. Oncotarget *6*, 33165–33177.

49. Liu, B.L., Robinson, M., Han, Z.Q., Branston, R.H., English, C., Reay, P., McGrath, Y., Thomas, S.K., Thornton, M., Bullock, P., et al. (2003). ICP34.5 deleted herpes simplex virus with enhanced oncolytic, immune stimulating, and anti-tumour properties. Gene Ther. *10*, 292–303.

50. Whelan, S.P., Ball, L.A., Barr, J.N., and Wertz, G.T. (1995). Efficient recovery of infectious vesicular stomatitis virus entirely from cDNA clones. Proc. Natl. Acad. Sci. USA *92*, 8388–8392.